Free Radical Research, May 2007; 41(5): 523–535

informa
healthcare

^{15}N-CIDNP investigations during tryptophan, *N*-acetyl-L-tryptophan, and melatonin nitration with reactive nitrogen species

M. LEHNIG[1] & M. KIRSCH[2,†]

[1]*Organische Chemie, Fachbereich Chemie, Universität Dortmund, Otto-Hahn-Strasse 6, D-44221 Dortmund, Germany, and* [2]*Institut für Physiologische Chemie, Universitätsklinikum Essen, Hufelandstr. 55, D-45122 Essen, Germany*

Accepted by Professor M. Davies

(Received 2 October 2006; in revised form 10 November 2006)

Abstract

Tryptophan and melatonin are nitrated by peroxynitrite; tryptophan residues in proteins are susceptible to attack by reactive nitrogen species. Nitrated tryptophan might therefore be used as a biomarker for the involvement of reactive species derived from nitrogen oxide in a variety of pathophysiological conditions. The radical character of the tryptophan (Trp) and *N*-acetyl-L-tryptophan (*N*-AcTrp) nitration with peroxynitrite is shown using ^{15}N-CIDNP. During the decay of peroxynitrite-^{15}N in the presence of Trp at pH 5 in the probe of a ^{15}N-NMR spectrometer, the ^{15}N-NMR signals of various nitrated tryptophans ($^{15}NO_2$-Trp) show emission (E). The effects are built up in radical pairs [Trp$^{\cdot}$, $^{15}NO_2^{\cdot}$]^{F} formed by diffusive encounters of radicals $^{15}NO_2^{\cdot}$ and Trp$^{\cdot}$ generated during decay of peroxynitrite-^{15}N in the presence of Trp. Similar ^{15}N-CIDNP effects are observed during reaction of Trp and/or *N*-AcTrp using the nitrating systems H$^{15}NO_3$, H$^{15}NO_4$ and H_2O_2/$^{15}NO_2^-$/HRP, which are also built up in radical pairs [Trp$^{\cdot}$, $^{15}NO_2^{\cdot}$]^{F}. During nitration of melatonin (Mel) with peroxynitrite-^{15}N and H$^{15}NO_4$, the ^{15}N-NMR signal of 4-nitromelatonin (4-$^{15}NO_2$-Mel) shows emission arising from radical pairs [Mel$^{\cdot}$, $^{15}NO_2^{\cdot}$]^{F} which are formed in an analogous manner.

Keywords: *Tryptophan, 6-nitrotryptophan, melatonin, peroxynitrite, reactive nitrogen species (RNS), nitrogen dioxide*

Abbreviations: *1, 3-methylindane; 2, 3-methyl-5-methoxyindane; A, enhanced absorption; AcOH, acetic acid;* c, *cage product; CIDNP, chemically induced dynamic nuclear polarization; E, emission;* e, *escape product; F, radical precursor;* g, g *value; HRP, horseradish peroxidase; Mel, melatonin (*N*-[2-(5-methoxy-1*H*-indol-3yl)ethyl]-acetamide; MetMb, Metmyoglobin; MPO, myeloperoxidase; N, no CIDNP effect;* N*-AcTrp,* N*-acetyl-L-tryptophan;* N*-AcTrp-NH$_2$,* N*-acetyl-L-tryptophan amide; NO$_2$-Mel, nitromelatonin; NO$_2$-*N*-AcTrp, nitro-*N*-acetyl-L-tryptophan; NO$_2$-Trp, nitrotryptophan; NO$_2$-Tyr, nitrotyrosine; RNS, reactive nitrogen species; S, singlet state*

Introduction

Peroxynitrite (O═NO—OH, pK 6.5–6.8) is known as an unstable intermediate during reaction of hydrogen peroxide (H_2O_2) with nitrous acid (HNO_2) [1]. In recent years, peroxynitrite—this term is commonly used for the acid-base equilibrium mixture of peroxynitrous acid (O═NO—OH) and peroxynitrite anion (O═NOO$^-$)—has received considerable attention as a putative cytotoxic agent in living organisms where it may be produced by recombination of endogenous nitric oxide (NO$^{\cdot}$) and superoxide anion ($O_2^{\cdot-}$) [2]. It isomerizes to nitrate or may react with L-tyrosine (Tyr) forming 3-nitrotyrosine (3-NO$_2$-Tyr) which is a useful marker of oxidants like peroxynitrite [3,4]. It also reacts with L-tryptophan (Trp) and

Correspondence: M. Lehnig, Fachbereich Chemie, Universität Dortmund, Otto-Hahn-Strasse 6, D-44221 Dortmund, Germany. Fax: 49 231 755 5363. E-mail: manfred.lehnig@uni-dortmund.de

†Physiologische Chemie, Universitätsklinikum Essen, Hufelandstr. 55, D-45122 Essen, Germany. Fax: 49 201 723 5943. E-mail: michael.kirsch@uni-duisburg-essen.de

ISSN 1071-5762 print/ISSN 1029-2470 online © 2007 Informa UK Ltd.
DOI: 10.1080/10715760601161445

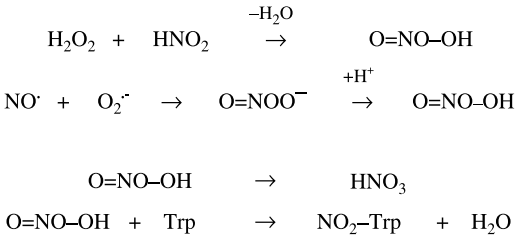

Scheme 1. Peroxynitrite formation, decay and tryptophan nitration reaction.

tryptophan residues in proteins to various nitrated tryptophans (NO_2-Trp), see Scheme 1 [5,6]. 6-Nitro-L-tryptophan (6-NO_2-Trp) which is the most important nitration product might be useful as a biomarker of endogeneous production of reactive nitrogen species (RNS) [6].

The mechanisms of the isomerization and nitration reactions were in discussion for a long time. A radical mechanism is generally accepted now (Scheme 2) [7]. The first step is an O—O bond homolysis to give hydroxyl radicals ($^{\cdot}OH$) and nitrogen dioxide ($NO_2^{\cdot}$). In the presence of CO_2, a decay reaction via a peroxynitrite-CO_2 adduct ($O{=}NO{-}OCO_2^-$) has been proposed leading to both $NO_2^{\cdot}$ and $CO_3^{\cdot-}$ [8]. In a second step, the radicals react by O^- transfer to NO_3^-.

The radical character of the $O{=}NO{-}OCO_2^-$ decay and the Tyr nitration has been proved by ^{15}N-CIDNP [9,10]. Tyrosinyl radicals $Tyr^{\cdot}$ are formed by H abstraction from Tyr. Recombination of radicals $NO_2^{\cdot}$ and $Tyr^{\cdot}$ gives 3-NO_2-Tyr (Scheme 2).

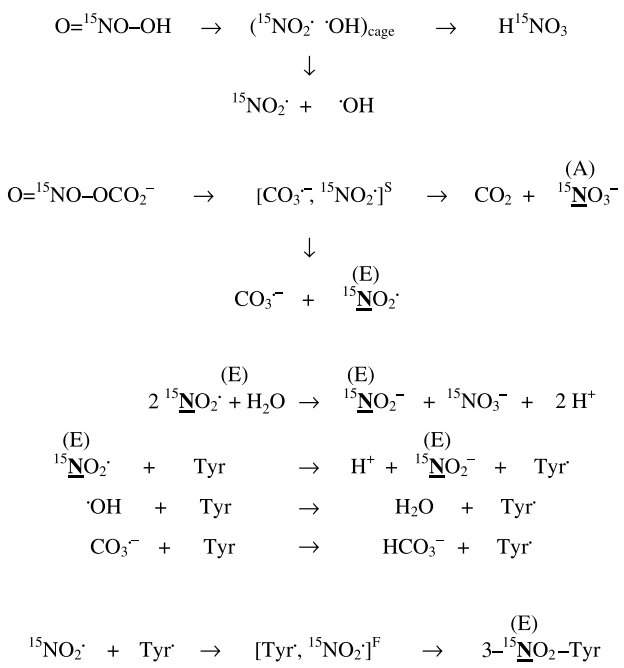

Scheme 2. ^{15}N-CIDNP during peroxynitrite-^{15}N isomerization and tyrosine nitration.

CIDNP is the appearance of emission (E) and enhanced absorption (A) signals in NMR spectra during the occurrence of fast radical reactions in the probe of a NMR spectrometer [11]. The unusual signal intensities indicate nuclear polarizations in the products of radical reactions. Following the radical pair theory of CIDNP, nuclear polarizations are built up in radical pairs formed by homolytic bond scission of diamagnetic compounds from singlet states (S pairs). They might also be generated in radical pairs formed by diffusive encounters of independently generated radicals (F pairs) [12]. CIDNP is used to prove the radical character of chemical reactions, particularly the product formation via radical pairs. If radicals are present during peroxynitrite decay and nitration reactions, the formation of S as well as of F pairs is expected. Nuclear polarizations are not generated in pairs of radicals with axial symmetry and degenerate orbitals like $HO^{\cdot}$, $O_2^{\cdot-}$, or $^{15}NO^{\cdot}$ [13]. Because of this, radical pairs $[HO^{\cdot}, {}^{15}NO_2^{\cdot}]^S$ formed by O—O bond scission of peroxynitrite do not lead to ^{15}N-CIDNP effects.

Nitrogen centered radicals are involved during peroxynitrite decay and nitration reactions. Therefore, it is convenient to apply ^{15}N-NMR spectroscopy. This requires the use of ^{15}N enriched compounds. ^{15}N-CIDNP effects which are expected from thermal reactions of $^{15}NO_2^{\cdot}$ and radicals $R^{\cdot}$ with $g(R^{\cdot}) > g(^{15}NO_2^{\cdot})$ are exemplified in Scheme 3 [12,14].

Radicals which react within the pairs give cage (*c*) products showing A(E) if arising from S(F) pairs. This allows to distinguish between S and F precursors. Radicals which do not react within the pairs form escape (*e*) products giving CIDNP patterns of opposite signs. An analysis of CIDNP effects allows the differentiation between product formation via *c* or *e* reactions, too.

A radical mechanism of the Trp nitration is likely—in analogy to the Tyr nitration—but has not yet been proved with CIDNP. The purpose of this report is to confirm the radical character of the tryptophan nitration by RNS using ^{15}N-CIDNP. The nitration of *N*-AcTyr has been investigated by various authors and will be considered, too. Under physiological conditions, peroxynitrite and the system H_2O_2/NO_2^-/peroxidase are the most important nitration systems which will be applied using horseradish peroxidase (HRP). For comparison, HNO_3 will be

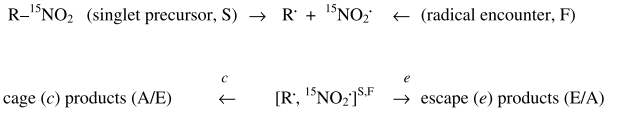

Scheme 3. ^{15}N-CIDNP effects from reactions of $^{15}NO_2^{\cdot}$ with radicals $R^{\cdot}$ assuming $g(R^{\cdot}) > g(^{15}NO_2^{\cdot})$. E: emission, A: enhanced absorption.

used as a well-known nitrating agent in strongly acidic media. The application of HNO_4 to *N*-AcTyp nitration at medium pH will complete this study [15]. In a further part, the nitration of the Trp derivative melatonin (*N*-[2-(5-methoxy-1*H*-indol-3yl)-ethyl]-acetamide; Mel) will be described, too. Mel is recognized as a scavenger of strong oxidants [16].

Materials and methods

^{15}N-CIDNP experiments with preformed and in situ *generated peroxynitrite-^{15}N*

Stock solutions of peroxynitrite-^{15}N (0.435 ± 0.01 M $O{=}{}^{15}NOO^-$) were prepared by reaction of *iso*-amylnitrite-^{15}N (0.0024 mol) with hydrogen peroxide (2 ml H_2O_2,1 M) in diethylene-triaminepentaacetic acid-free solutions and purified (six times solvent extraction with *n*-hexane, removal of excess H_2O_2 by passing over MnO_2, N_2-purging) [17], divided into 200-μl aliquots in 1-ml Eppendorf vials and stored at 194 K in the dark. The reaction mixtures were prepared in 10-mm NMR tubes by adding peroxynitrite-^{15}N to the frozen solvent (H_2O/D_2O: 9/1) containing phosphate buffer (0.3 M), if required, $NaHCO_3$ (0.05 M) and Trp or *N*-AcTrp (0.05 M) at 268 K. The final pH after mixing was 7.5. The tubes were quickly transferred into the probe of the ^{15}N-NMR spectrometer (Bruker DPX-300) and locked (internal lock: D_2O). One minute after mixing of the reactants, the first ^{15}N-NMR spectrum was taken by using single pulses with pulse angles of 90°. This procedure was repeated every minute until the reaction was completed. For detecting reaction products, ^{15}N-NMR spectra were taken with several pulses at room temperature.

For generating peroxynitrite-^{15}N *in situ*, a solution of $Na^{15}NO_2$ (0.05 M) in H_2O/D_2O (9:1) containing phosphate buffer (0.3 M) and, when needed, $NaHCO_3$ (0.05 M) and Trp or *N*-AcTrp (0.05 M) was prepared in 10 mL tubes at pH 5, and a single ^{15}N-NMR spectrum was taken using a 90° pulse. After that, the tube was replaced, and H_2O_2 (1 M) was added to the solution. ^{15}N-NMR spectra were then taken every 1–5 min until the reaction was completed.

^{15}N-CIDNP experiments with the systems $H_2O_2/{}^{15}NO_2^-$/HRP, $H^{15}NO_3$, and $H^{15}NO_4$

Solutions of HRP (20 μM), H_2O_2 (1 M), $Na^{15}NO_2$ (0.05 M) and *N*-AcTrp were prepared at pH 7 [18]. Spectra were taken as described above. Nitration of *N*-AcTrp (0.05 M) with $H^{15}NO_3$ was performed by adding *N*-AcTrp to a solution of $H^{15}NO_3$ (0.5 M) in AcOH with 10% D_2O [19]. $H^{15}NO_4$ was prepared *in situ* by adding H_2O_2 (1 M) to a solution of $Na^{15}NO_2$ (0.15 M) at pH 2 [20]. After about 2 min, *N*-AcTrp (0.05 M) was added [15].

Materials and solutions

It was taken care to exclude possible contamination by CO_2 and transition metal ions. The following procedures were performed under nitrogen and at reduced incident light. Doubly distilled water was bubbled (21 min^{-1}) with nitrogen (5.0) at room temperature for 20 min and was then treated with the heavy metal ion scavenger resin Chelex 100 (0.5 g in 10 ml) by gently shaking for 18 h in the dark. After separation from the resin by low-speed centrifugation for 5 min and careful decanting, the water was again bubbled with nitrogen for 20 min.

$Na^{15}NO_2$ and *iso*-amylnitrite-^{15}N were purchased from Aldrich/Isotec Inc. (Taufkirchen, Germany). HNO_3 was 9.4 M in H_2O and labelled with 60.3 atom% ^{15}N. All other chemicals were from Sigma (Deisenhofen, Germany) and were of the highest purity available.

Calculation of ^{15}N chemical shifts

Isotropic absolute shielding constants were calculated using the GIAO protocol at the DFT/aug-cc-pVDZ/DFT/aug-cc-pVDZ level of theory. During these calculations solvation corrections (CH_3CN for nitrobenzol, H_2O for all others) with the CPCM solvation model were performed at the same level of theory [21].

Results and discussion

^{15}N-CIDNP during nitration of N-*AcTrp with $H^{15}NO_3$ in AcOH*

Nitration of Trp and its derivatives *N*-AcTrp and *N*-AcTrp-NH_2 with RNS has thoroughly been studied [6,22,23], see Table I. It mainly occurs at the 6-position of the indole system, leading to 6-NO_2-Trp, 6-NO_2-*N*-AcTrp, and 6-NO_2-*N*-AcTrp-NH_2. Besides, nitration at the 1-, 4-, 5- and 7- positions are reported (Figure 1). Aromatic compounds react with nitric acid in a non-radical way, if toluene and less activated compounds are used. Electron rich aromatic systems are nitrated via radicals in a nitrous acid catalysed path which can be proved using ^{15}N-CIDNP [14,26]. Indole derivatives are nitrated at various ring positions [27]. During reaction of *N*-AcTrp-NH_2 in AcOH, nitration at the 4-, 6- and 7-position are reported [25].The nitration mechanism of indoles with nitric acid has not yet been studied.

During reaction of $H^{15}NO_3$ with *N*-AcTrp in AcOH, a ^{15}N-NMR spectrum was taken which is shown in Figure 2(A), details of the reaction are given in Table II. Besides the ^{15}N-NMR signal at $\delta = -15$ ppm due to $H^{15}NO_3$, emission signals at $\delta = -10$, 2, 4, 18 and 19 ppm are observed which are caused by nitration products of *N*-AcTrp. After reaction, a spectrum was taken with 167 scans and is given in Figure 2(B).

Table I. Nitration products of Trp and its derivatives with RNS [6]⋆.

System	Trp	Nitrated products	Ref.
$O{=}NOO^-$	Trp	6-NO_2-Trp 5-NO_2-Trp 4- or 7-NO_2-Trp (minor)	[22]
$O{=}NOO^-$ (0.5 mM)	Trp	6-NO_2-Trp	[23]
(5–10 m M)	Trp	6-NO_2-Trp (major) + other NO_2-Trps	
$O{=}NOO^-$	*N*-AcTrp	1-NO_2-*N*-AcTrp 6-NO_2-*N*-AcTrp	[5]
H_2O_2/NO_2^-/MPO	*N*-AcTrp	1-NO_2-*N*-AcTrp 6-NO_2-*N*-AcTrp	[5]
H_2O_2/NO_2^-/MetMb	Trp	4-NO_2-Trp 5-NO_2-Trp 6-NO_2-Trp	[24]
H_2O_2/NO_2^-/HRP or HNO_3 in AcOH	*N*-AcTrp-NH_2	1-NO_2-*N*-AcTrp-NH_2† 4-NO_2-*N*-AcTrp-NH_2 6-NO_2-*N*-AcTrp-NH_2 7-NO_2-*N*-AcTrp-NH_2	[25]
$O{=}NOO^-$	Mel	4-NO_2-Mel 6-NO_2-Mel	[16]

⋆ MPO, myeloperoxidase; *N*-AcTrp-NH_2, *N*-acetyl-L-tryptophan amide; MetMb, metmyoglobin; † Not formed with HNO_3.

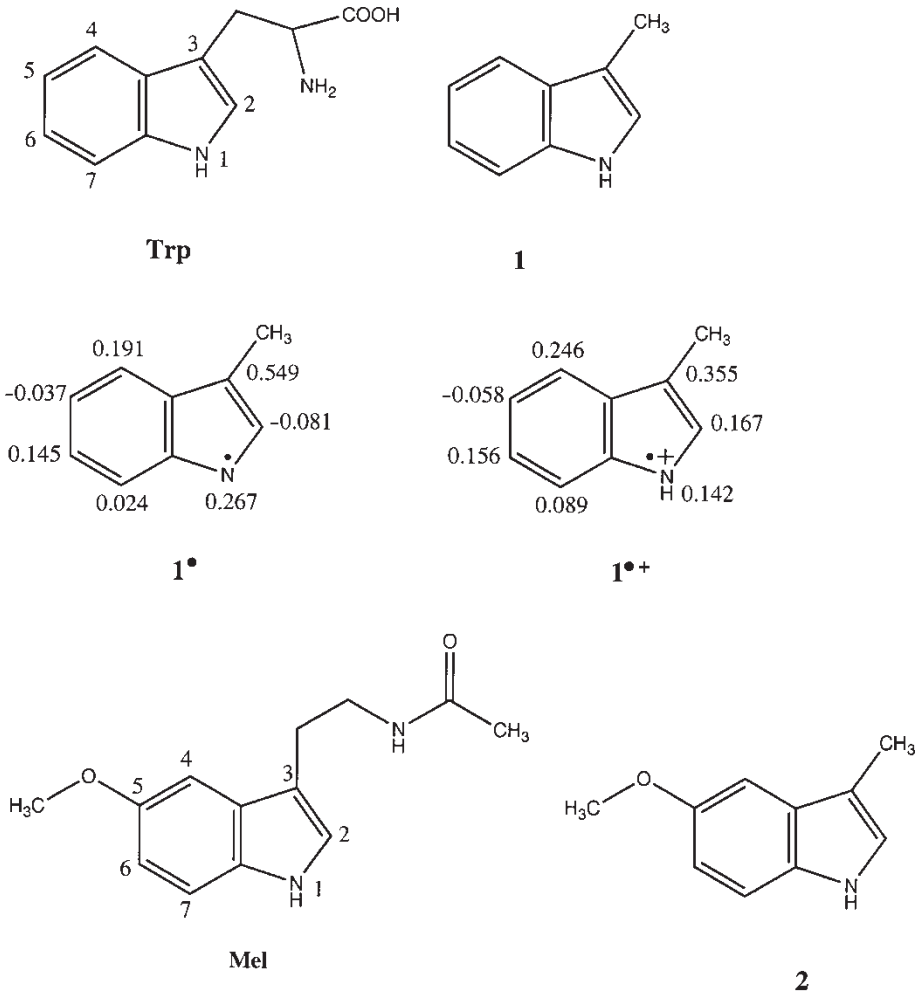

Figure 1. Indane derivatives and spin densities in radicals $\mathbf{1}^{\cdot}$ and radical cations $\mathbf{1}^{\cdot+}$. Trp, Tryptophan; **1**, 3-Methylindane; Mel, Melatonin; **2**, 3-Methyl-5-methoxyindane.

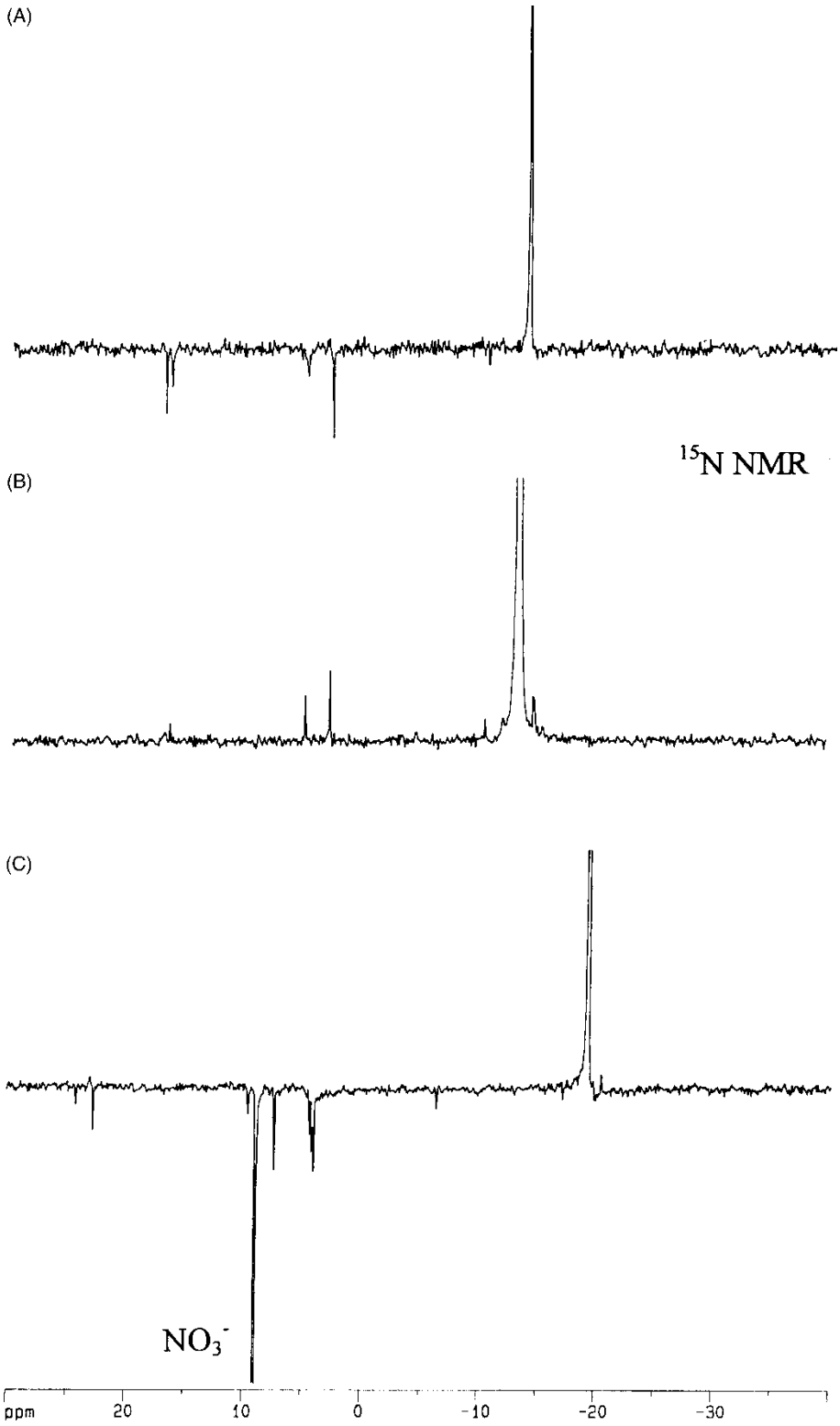

Figure 2. (A) ^{15}N-NMR spectrum during reaction of $H^{15}NO_3$ with *N*-AcTrp in AcOH/D_2O 2 min after mixing the reactants (1 scan), (B) 100 min later (167 scans). (C) ^{15}N-NMR spectrum during reaction of $H^{15}NO_4$ with *N*-AcTrp at pH 2 in H_2O/D_2O 2 min after mixing the reactants (1 scan).

The signals of the nitration products show weak absorption signals indicating the occurrence of ^{15}N-CIDNP during reaction. Reactions leading to the ^{15}N-CIDNP effects are given in Scheme 3. Analogous effects have been observed during reaction of $H^{15}NO_3$ with electron-rich aromatics, especially with tyrosine and *N*-acetyl-L-tyrosine (*N*-AcTyr) [9,19], which have similar redox potentials (Trp: 1.015 V, Tyr: 0.93 V at pH 7 [28]), and have been explained in an analogous manner. The effects are built up in radical pairs

Table II. ^{15}N-CIDNP during nitration of *N*-AcTrp with $H^{15}NO_3$ and $H^{15}NO_4$ at 298 K.

System	^{15}N-NMR signals	CIDNP⋆
$H^{15}NO_3$ (0.5 M), *N*-AcTrp (0.05 M), AcOH, Ph < 1 (Figure 2a)	−15 ($H^{15}NO_3$)	N
	−10 (2-$^{15}NO_2$-*N*-AcTrp)	E
	2 (6-$^{15}NO_2$-*N*-AcTrp)†	E
	4 (4-$^{15}NO_2$-*N*-AcTrp)	E
	18 (3-$^{15}NO_2$-*N*-AcTrp)‡	E
	19 (3-$^{15}NO_2$-*N*-AcTrp)‡	E
$H^{15}NO_4$ ¶, *N*-AcTrp (0.05 M) pH 2 (Figure 2c)	−20 ($H^{15}NO_4$)	A
	−7 (2-$^{15}NO_2$-*N*-AcTrp)	E
	3 (6-$^{15}NO_2$-*N*-AcTrp)	E
	7 (4-$^{15}NO_2$-*N*-AcTrp)	E
	9 ($^{15}NO_3^-$)	N

⋆E: emission, A: enhanced absorption, N: no CIDNP; †The signals might also be assigned to 5- and 7-$^{15}NO_2$-*N*-AcTrp, see Table III; ‡Two diastereomeric configurations; ¶Generated *in situ* by reaction of $Na^{15}NO_2$ (0.15 M) with H_2O_2 (1 M).

[*N*-AcTrp$^{\cdot+}$, $^{15}NO_2^{\cdot}$]^F generated by encounters of radicals $^{15}NO_2^{\cdot}$ and radical cations *N*-AcTrp$^{\cdot+}$ which are formed independently. Reaction between $H^{15}NO_3$ and $H^{15}NO_2$ generates $^{15}NO_2^{\cdot}$. *N*-AcTrp$^{\cdot+}$ is formed by oxidation with $H^{15}NO_2$ or, more probably, some reactive intermediate like $^{15}NO^+$ which is easily formed at strongly acidic conditions.

The emission-type effect in the ^{15}N-NMR signals of $^{15}NO_2$-*N*-AcTyp is explained using the observed *g* values of $NO_2^{\cdot}$ (2.000) and Trp$^{\cdot}$ (2.003) [29,30], see Schemes 3 and 4. The reported pK value of 4.3 for Trp$^{\cdot}$ indicates that the protonated form of the radical, *N*-AcTrp$^{\cdot+}$, should be present under the reaction conditions [31]. For assigning the emission signals to distinct nitration products, ^{15}N chemical shifts have been quantum-chemically calculated [21]. For simplicity, 3-methylindane **1** has been chosen as a model compound (Figure 1). The results are listed in Table III. A spin density distribution for the radical cation of **1**, **1**$^{\cdot+}$, is added, showing that radical recombination reactions are possible at different ring positions [32]. At first, it should be noted that 1-$^{15}NO_2$-*N*-AcTrp is obviously not formed, as the corresponding ^{15}N-NMR signal is missing, in agreement with data of Ref. [25]. The small emission signal at $\delta = -10$ ppm might be due to 2-$^{15}NO_2$-*N*-AcTrp. The strong emission signals at $\delta = 1$ ppm and $\delta = 4$ ppm are assigned to 5-, 6-, 7-$^{15}NO_2$-*N*-AcTrp and 4-$^{15}NO_2$-*N*-AcTrp, respectively, which are the main products, in accordance with the literature, see Table I. The narrow doublet at $\delta = 18$ ppm and $\delta = 19$ ppm is assigned to 3-$^{15}NO_2$-*N*-AcTrp which is formed in two diastereomeric configurations, in accordance with the formation of cyclohexadienone-like intermediates observed during nitration of tyrosine and related compounds [9,10,14,19].

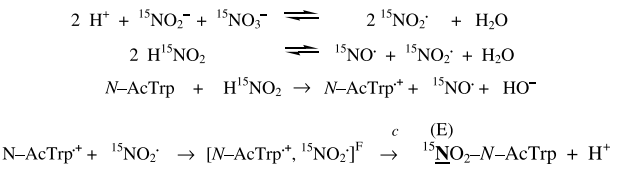

Scheme 4. ^{15}N-CIDNP during nitration of *N*-AcTrp with $H^{15}NO_3$.

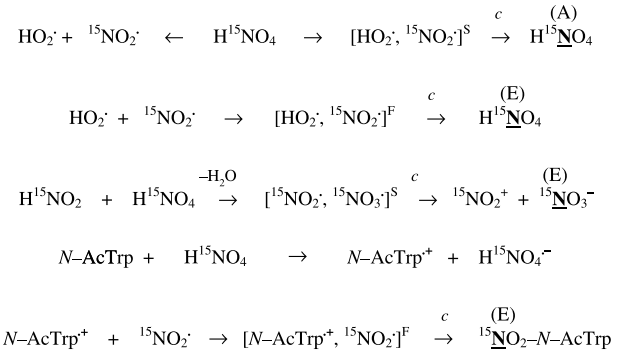

Scheme 5. ^{15}N-CIDNP during nitration of *N*-AcTrp with $H^{15}NO_4$.

Table III. Quantum-chemically calculated isotropic absolute shielding constants and ^{15}N chemical shifts (δ, in ppm against nitrobenzene-^{15}N).

	Isotropic shielding constants⋆		Isotropic chemical shifts	
Molecule	B1LYP	B3LYP	B1LYP	B3LYP
Nitrobenzene	−125.2	−121.5	0.0	0.0
NO_3^-	−134.9	−130.2	9.7	8.7
O_2NOOH	−105.6	−105.8	−19.6	−15.7
1- NO_2-**1**	−81.7	−77.6	−3.5	−43.9
2- NO_2-**1**	−110.7	−106.2	−14.5	−15.3
3- NO_2-**1**	−149.0	−149.0	23.8	27.5
4- NO_2-**1**	−131.9	−127.7	6.7	6.2
5- NO_2-**1**	−127.1	−122.9	1.9	1.4
6- NO_2-**1**	−126.9	−122.7	1.7	1.2
7- NO_2-**1**	−126.9	−122.6	1.7	1.1

⋆Isotropic absolute shielding constants were calculated using the GIAO protocol at the DFT/aug-cc-pVDZ//DFT/aug-cc-pVDZ level of theory. During these calculations solvation corrections (CH_3CN for nitrobenzol, H_2O for all others) with the CPCM solvation model were performed at the same level of theory [21].

Table IV. ^{15}N-CIDNP during nitration of Trp and *N*-AcTrp with peroxynitrite-^{15}N and the system $H_2O_2/^{15}NO_2^-$/HRP at 298 K.

System	^{15}N-NMR signals	CIDNP*
Peroxynitrite-^{15}N (0.03 M)	8 ($^{15}NO_3^-$)	N
Trp (0.05 M), 268 K, pH 7.5	242 ($^{15}NO_2^-$)	N
Peroxynitrite-$^{15}N^{\dagger}$, Trp (0.05 M),	−20 ($H^{15}NO_4$)	N
$NaHCO_3$ (0.05 M), pH 5	1 (6-$^{15}NO_2$-Trp)‡	E
(Figure 3)	4 (4-$^{15}NO_2$-Trp)	E
	8 ($^{15}NO_3^-$)	A
	15 (3-$^{15}NO_2$-Trp)¶	E
	16 (3-$^{15}NO_2$-Trp)¶	E
	242 ($^{15}NO_2^-$)§	E
Peroxynitrite-$^{15}N^{\dagger}$, *N*-AcTrp	−19 ($H^{15}NO_4$)	E
(0.05 M), pH 5 (Figure 4a)	−10 (2-$^{15}NO_2$-*N*-AcTrp)	E
	0–8 ($^{15}NO_2$-*N*-AcTrp)$^{\|}$	E
	8 ($^{15}NO_3^-$)	N
	242 ($^{15}NO_2^-$)§	N
HRP (20 μM), H_2O_2 (1 M),	8 ($^{15}NO_3^-$)	N
$Na^{15}NO_2$ (0.05 M), *N*-AcTrp	0–8 ($^{15}NO_2$-*N*-AcTrp)$^{\|}$	E
(0.05 M), pH 7 (Figure 4b,c)	242 ($^{15}NO_2^-$)§	N

* E: emission, A: enhanced absorption, N: no CIDNP; † Generated *in situ* by reaction of $Na^{15}NO_2$ (0.05 M) with H_2O_2 (1 M); ‡ The signals might be assigned to 5- and 7-$^{15}NO_2$-Trp, too; ¶ Two diastereoisomeric configurations; § Not shown in Figures 3 and 4; ‖ Assigned to 4-, 5-, 6- and/or 7-$^{15}NO_2$-*N*-AcTrp.

^{15}N-CIDNP during nitration of N-AcTrp with $H^{15}NO_4$

Peroxynitric acid is able to nitrate electron-rich aromatics at pH 2–3 [15]. During reaction of $H^{15}NO_4$ with *N*-AcTrp at pH 2, the ^{15}N-NMR signals of $^{15}NO_3^-$ and of $H^{15}NO_4$ appear in emission and in enhanced absorption, respectively. Emission is observed in additional signals (Figure 2(C), Table II), which might be due to 2-$^{15}NO_2$-*N*-AcTrp ($\delta = -7$ ppm), to 5-, 6- and 7-$^{15}NO_2$-*N*-AcTrp ($\delta = 3$ ppm) and to 4-$^{15}NO_2$-*N*-AcTrp ($\delta = 7$ ppm), in analogy to the reaction of *N*-AcTrp with $H^{15}NO_3$. The signals at $\delta \sim 25$ ppm point to some unidentified products. The effects in the ^{15}N-NMR signals of $^{15}NO_3^-$ and $H^{15}NO_4$ are explained by reactions of $H^{15}NO_4$ with $H^{15}NO_2$ and by decay of $H^{15}NO_4$ [15], those in $^{15}NO_2$-*N*-AcTrp by reactions of *N*-AcTrp$^{\cdot+}$ and $^{15}NO_2^{\cdot}$ in radical pairs [*N*-AcTrp$^{\cdot+}$, $^{15}NO_2^{\cdot}$]^F, see Scheme 5. Radical cations of *N*-AcTrp are formed by oxidation with $H^{15}NO_4$ or some RNS like $^{15}NO^+$, $^{15}N_2O_3$, or $^{15}NO_3^{\cdot}$ which are present during the decay of $H^{15}NO_4$.

^{15}N-CIDNP during nitration of Trp with preformed and in situ generated peroxynitrite-^{15}N

Reactions of peroxynitrite with Trp and *N*-AcTrp have thoroughly been studied [5,22,23], see Table I. The most important reaction is nitration at the 6-position of the indole system leading to 6-NO_2-Trp or 6-NO_2-*N*-AcTrp. Nitrations at the ring positions 1, 4, 5 and 7 are also reported. Besides, a few additional products are formed which have not been listed in Table I and will not be discussed in the following. For taking ^{15}N-NMR spectra at pH 7, the reaction of peroxynitrite-^{15}N with Trp was performed at 268 K, because CIDNP effects can only be observed, if reaction times are similar to nuclear relaxation times which are in the order of minutes [33]. As the protonated form of peroxynitrite decays with a rate of $1.3\,s^{-1}$ at 298 K [34], it is impossible to observe ^{15}N-CIDNP at physiological pH values and room temperature with preformed peroxynitrite. At 268 K and pH 7.5, the decay rate of peroxynitrite is about $0.0025\,s^{-1}$ [35] giving reaction times of 10 min [10]. During the reaction, ^{15}N-NMR signals of $^{15}NO_2^-$ and $^{15}NO_3^-$ appear within 3 min indicating the end of the reaction at that time. ^{15}N-CIDNP effects are not observed. Details of the reaction conditions are given in Table IV. The results agree with those reported during the peroxynitrite-^{15}N decay in the absence of Trp [9,10]. At peroxynitrite concentrations of 0.03 M, the reaction of peroxynitrite with Trp is slower than the induced decomposition reaction of peroxynitrite taking place under the given conditions [10].

The reported reactions of peroxynitrite with Trp have been performed at peroxynitrite concentrations of about 1 mM which are too small for CIDNP experiments because of the low sensitivity of ^{15}N-NMR spectroscopy. This difficulty was circumvented by generating peroxynitrite-^{15}N *in situ* using the Baeyer-Villiger reaction [1], see Figure 3 and Table IV. At pH 5, it is finished after about 10 min using $[Na^{15}NO_2] = 0.05$ M and $[H_2O_2] = 1$ M.

A ^{15}N-NMR spectrum of a solution of $Na^{15}NO_2$ and Trp in H_2O/D_2O in the presence of $NaHCO_3$ is given in Figure 3(A). The signal of $Na^{15}NO_2$ at $\delta = 242$ ppm is not shown in Figure 3. After adding H_2O_2 to the solution, strong absorption and emission

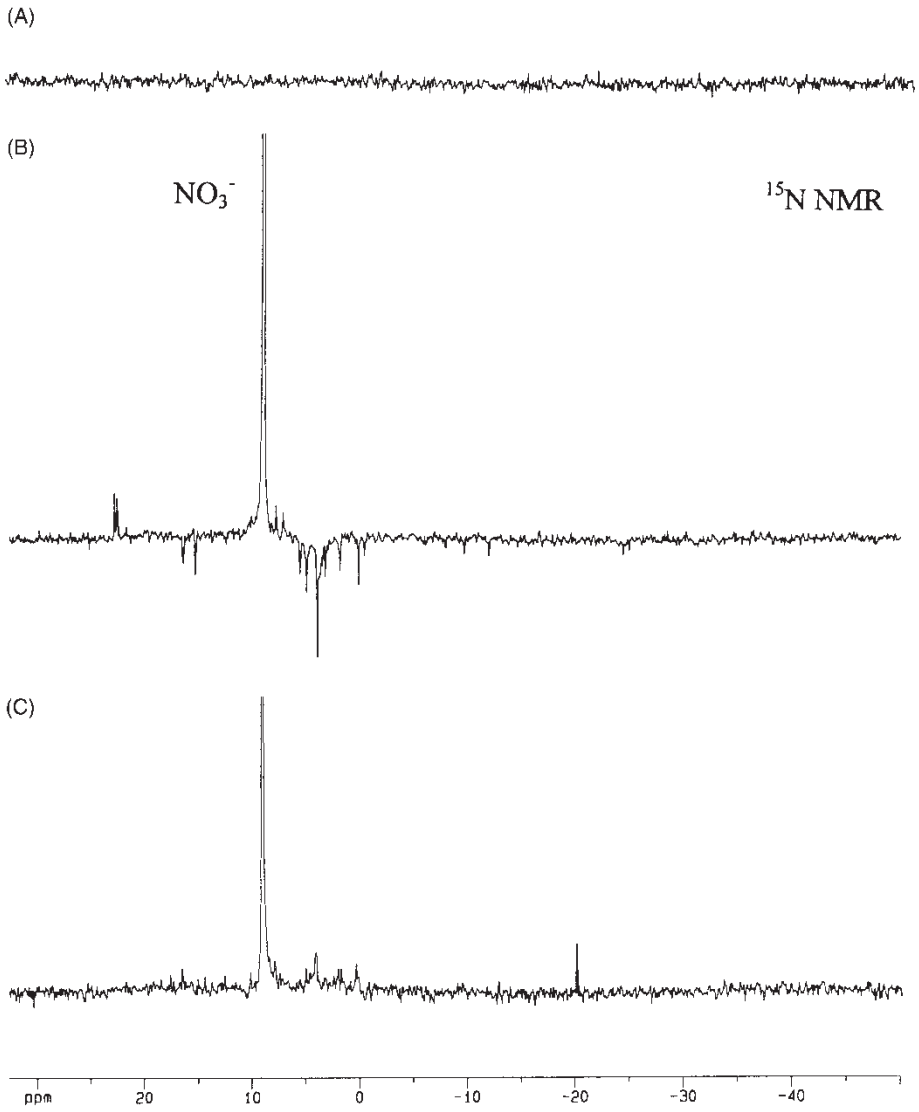

Figure 3. ^{15}N-NMR spectra of $Na^{15}NO_2$, $NaHCO_3$ and Trp at pH 5 in H_2O/D_2O (A) before adding H_2O_2 (1 scan), (B) 2 min after adding H_2O_2 (1 scan), (C) 100 min later (900 scans).

signals are observed (Figure 3(B), Table IV). After reaction, the spectrum given in Figure 3(C) was taken using 900 scans. Besides the ^{15}N-NMR signals at $\delta = 9$ ppm and $\delta = -20$ ppm due to $^{15}NO_3^-$ and $H^{15}NO_4$, it shows signals at $\delta = 1$ ppm and $\delta = 4$ ppm which are assigned to nitration products of Trp. The assignment is supported by chemical shift calculations of nitrated 3-methylindole (Table III), and the assignment during reaction of Trp with $H^{15}NO_3$, see above. The signal at $\delta = 4$ ppm is then due to 4-$^{15}NO_2$-Trp, the signal at $\delta = 1$ ppm to 5-, 6- and 7-$^{15}NO_2$-Trp. Signals which might be caused by 1-, 2- and 3-$^{15}NO_2$-Trp are not detected.

$$^{15}NO_2^{\cdot} + \text{Trp} \rightarrow H^+ + {}^{15}NO_2^{-} + \text{Trp}^{\cdot}$$

$$^{\cdot}OH + \text{Trp} \rightarrow H_2O + \text{Trp}^{\cdot}$$

$$CO_3^{\cdot-} + \text{Trp} \rightarrow CO_3^{2-} + \text{Trp}^{\cdot+}$$

$$\text{Trp}^{\cdot} + {}^{15}NO_2^{\cdot} \rightarrow [\text{Trp}^{\cdot}, {}^{15}NO_2^{\cdot}]^F \xrightarrow{c} {}^{15}\underline{N}O_2\text{–Trp (E)}$$

$$\text{Trp}^{\cdot+} + {}^{15}NO_2^{\cdot} \rightarrow [\text{Trp}^{\cdot+}, {}^{15}NO_2^{\cdot}]^F \xrightarrow{c} {}^{15}\underline{N}O_2\text{–Trp} + H^+ \text{ (E)}$$

Scheme 6. ^{15}N-CIDNP during reaction of peroxynitrite-^{15}N with Trp and Trp derivatives.

During the reaction, the signal of $^{15}NO_3^-$ at $\delta = 8$ ppm shows enhanced absorption. Additionally, the ^{15}N-NMR signal of $^{15}NO_2^-$ at $\delta = 242$ ppm which is not given in Figure 3 shows emission. The ^{15}N-CIDNP effects are also observed in the absence of Trp and are generated in radical pairs $[CO_3^{\cdot-}, {}^{15}NO_2^{\cdot}]^S$ formed during decay of $O{=}{}^{15}NO{-}OCO_2^-$ [10], see Scheme 2. $H^{15}NO_4$ ($\delta = -20$ ppm) is also formed in the absence of Trp [19]. The emission signals between $\delta = 20$ ppm and $\delta = -15$ ppm are caused by additional reaction products. The intensive emission signals at $\delta = 4$ ppm and $\delta = 1$ ppm are due to

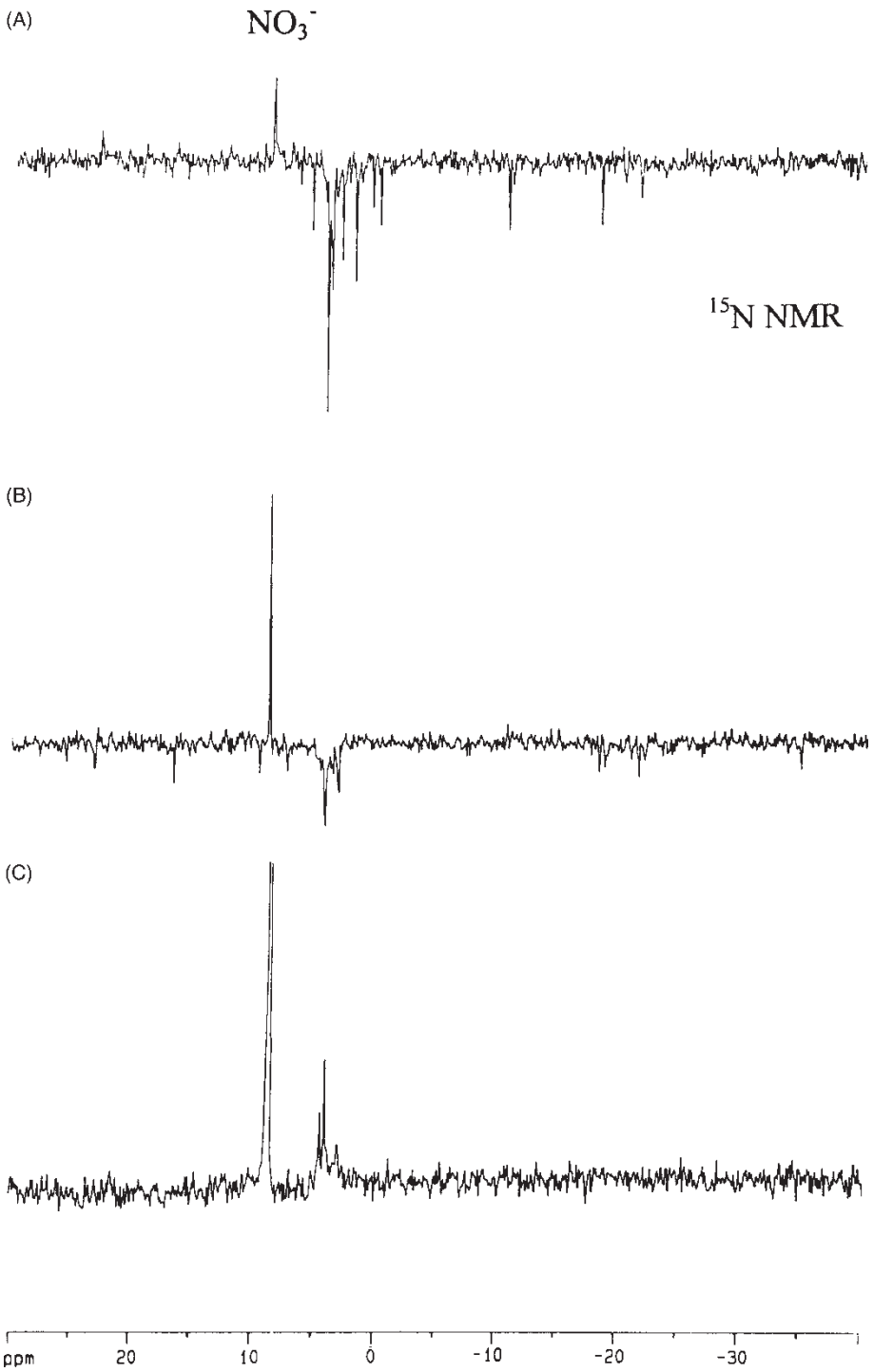

Figure 4. ^{15}N-NMR spectra of *N*-AcTrp in H_2O/D_2O (A) during reaction of peroxynitrite-^{15}N at pH 5 2 min after mixing the reactants (1 scan), (B) during reaction with H_2O_2, $Na^{15}NO_2$ and HRP at pH 7 2 min after mixing the reactants (20 scans, delay time 20 s), (C) 1000 min later (7421 scans).

4-$^{15}NO_2$-Trp and 5-, 6- and/or 7-$^{15}NO_2$-Trp. The signals at $\delta = 15$ ppm and $\delta = 16$ ppm are assigned to the unstable *ipso* substitution products 3-$^{15}NO_2$-Trp. One of the weak signals around $\delta = -10$ ppm might be due to 2-$^{15}NO_2$-Trp. A signal at $\delta \sim -45$ ppm which might point to the formation of 1-$^{15}NO_2$-Trp is not observed. Two enhanced absorption signals at $\delta \sim 22$ ppm could not be assigned.

The occurrence of ^{15}N-CIDNP proves the radical mechanism of the $^{15}NO_2$-Trp formation. Radicals $Trp^{\cdot}$ or radical cations $Trp^{\cdot+}$ are generated by reaction of $^{15}NO_2^{\cdot}$ or $CO_3^{\cdot-}$ with Trp [5,29], see Scheme 6. Polarized $^{15}NO_2$-Trp is then formed by recombination

of $Trp^{\bullet}$ or $Trp^{\bullet+}$ with $^{15}NO_2^{\bullet}$ in radical pairs $[Trp^{\bullet}, {}^{15}NO_2^{\bullet}]^F$ or $[Trp^{\bullet+}, {}^{15}NO_2^{\bullet}]^F$.

Radicals $^{15}NO_2^{\bullet}$, $^{\bullet}OH$, and $CO_3^{\bullet-}$ are formed during decay of peroxynitrite-^{15}N and the peroxynitrite-^{15}N-CO_2 adduct (Scheme 1) giving radicals $Trp^{\bullet}$ or radical cations $Trp^{\bullet+}$. The emission-type effect in the ^{15}N-NMR signals of $^{15}NO_2$-Trp is explained using the observed g values of $NO_2^{\bullet}$ (2.000) and $Trp^{\bullet}$ (2.003) [29,30], see Scheme 2. The reported pK value of 4.3 for $Trp^{\bullet}$ indicates that $Trp^{\bullet}$ and $Trp^{\bullet+}$ should be present under the reaction conditions (pH 5) [31]. As $Trp^{\bullet}$ and $Trp^{\bullet+}$ should have similar spin densities at the indole ring positions [32], see Figure 1, the product yields of the different Trp nitraton products should be similar, too, and do not allow distinction between $Trp^{\bullet}$ and $Trp^{\bullet+}$ as free radical intermediates.

^{15}N-CIDNP experiments have also been performed in CO_2-free solutions during reaction of peroxynitrite with *N*-AcTrp, see Figure 4(A) and Table IV. The ^{15}N-CIDNP pattern looks similarly as that observed in the presence of CO_2. It is explained in an analogous manner as described (Scheme 4). The enhanced absorption of the ^{15}N-NMR signal due to $^{15}NO_3^-$ is missing (Scheme 2), and the ^{15}N-NMR signal of $H^{15}NO_4$ shows emission.

^{15}N-CIDNP during nitration of N-*AcTrp with the system $H_2O_2/^{15}NO_2^-$/HRP*

It has been shown that ^{15}N-CIDNP observed in acidic medium is caused by reactions of nitrogen dioxide with independently generated tryptophanyl radicals or radical cations in radical pairs $[Trp^{\bullet}, {}^{15}NO_2^{\bullet}]^F$ and/or $[Trp^{\bullet+}, {}^{15}NO_2^{\bullet}]^F$. For confirming this at physiological pH values, radicals $^{15}NO_2^{\bullet}$ were generated from $^{15}NO_2^-$ and H_2O_2 in the presence of HRP. It is well-known that Trp, *N*-AcTrp and *N*-AcTrp-NH_2 are nitrated by H_2O_2/NO_2^- in the presence of various peroxidases, see Table I [6,24,25]. Figure 4(B) shows a ^{15}N-NMR spectrum taken during reaction of H_2O_2 with $Na^{15}NO_2^-$ at pH 7 in the presence of HRP. It also shows emission lines in the region between $\delta = -25$ ppm and $\delta = 20$ ppm indicating the formation of $^{15}NO_2$-*N*-AcTrp by recombination of $^{15}NO_2^{\bullet}$ with radicals *N*-$AcTrp^{\bullet}$ during the reaction [36,37]. The most intensive signals between $\delta = 2$ ppm and $\delta = 5$ ppm might be assigned to 4-, 5-, 6- and 7 -$^{15}NO_2$-*N*-AcTrp again. They are also observed after reaction in a spectrum taken with 7421 scans (Figure 4(C)). A possible reaction mechanism is given in Scheme 7.

$$\begin{aligned}
&\text{HRP} + H_2O_2 \rightarrow \text{Compound I} + H_2O\\
&\text{Compound I} + {}^{15}NO_2^- \rightarrow \text{Compound II} + {}^{15}NO_2^{\bullet}\\
&\text{Compound II} + {}^{15}NO_2^- \rightarrow \text{HRP} + {}^{15}NO_2^{\bullet}\\
&{}^{15}NO_2^{\bullet} + N\text{–AcTrp} \rightarrow H^+ + {}^{15}NO_2^- + N\text{–AcTrp}^{\bullet}\\
&N\text{–AcTrp}^{\bullet} + {}^{15}NO_2^{\bullet} \rightarrow [N\text{–AcTrp}^{\bullet}, {}^{15}NO_2^{\bullet}]^F \xrightarrow{c} {}^{15}\underline{N}O_2\text{–}N\text{–AcTrp (E)}
\end{aligned}$$

Scheme 7. ^{15}N-CIDNP during reaction of H_2O_2 and $Na^{15}NO_2$ with *N*-AcTrp in the presence of HRP.

Table V. ^{15}N-CIDNP during nitration of Mel with RNS at 298 K.

System	^{15}N-NMR signals	CIDNP⋆
Peroxynitrite-^{15}N†, Mel (0.05 M), pH 5 (Figure 5b)	−19 ($H^{15}NO_4$)	E
	6 (4-$^{15}NO_2$-Mel)	E
	8 ($^{15}NO_3^-$)	N (A)‡
	16 (not assigned)¶	E
Peroxynitrite-^{15}N†, Mel (0.05 M), $NaHCO_3$ (0.05 M), pH 5 (Figure 5b)	−19 ($H^{15}NO_4$)	E
	6 (4-$^{15}NO_2$-Mel)	E
	8 ($^{15}NO_3^-$)	A
	22 (not assigned)¶	E
$H^{15}NO_4$§, Mel (0.05 M), pH 2 (Figure 5c)	−20 ($H^{15}NO_4$)	A
	6 (4-$^{15}NO_2$-Mel)	E
	8 ($^{15}NO_3^-$)	E

⋆ E: emission, A: enhanced absorption, N: no CIDNP; † Generated *in situ* by reaction of $Na^{15}NO_2$ (0.05 M) with H_2O_2 (1 M); ‡ The signal is slightly enhanced because traces of CO_2 cause a decomposition of the peroxynitrite-^{15}N in part via the CO_2 adduct; ¶ 3- or 5-$^{15}NO_2$-Mel (see Table VI); § Generated *in situ* by reaction of $Na^{15}NO_2$ (0.15 M) with H_2O_2 (1 M).

^{15}N-CIDNP during reaction of Mel with peroxynitrite-^{15}N and $H^{15}NO_4$

Nitration of melatonin (Mel) by peroxynitrite leads to 4-nitromelatonin (4-NO_2-Mel) as the main product and 6-nitromelatonin (6-NO_2-Mel) as a side product [16]. In the following, ^{15}N-CIDNP studies will be described using peroxynitrite-^{15}N and $H^{15}NO_4$ as nitrating agents.

During reaction of Mel with peroxynitrite-^{15}N in the absence of $NaHCO_3$, a spectrum was taken shown in Figure 5(A) and described in Table V. An emission

Table VI. Quantum-chemically calculated isotropic absolute shielding constants and ^{15}N chemical shifts (δ, in ppm against nitrobenzene-^{15}N).

	Isotropic shielding constants⋆		Isotropic chemical shifts	
Molecule	B1LYP	B3LYP	B1LYP	B3LYP
Nitrobenzol	−125.2	−121.5	0.0	0.0
1- NO_2-**2**	−80.3	−76.2	−44.9	−45.3
2- NO_2-**2**	−112.9	−108.5	−12.3	−13.0
3- NO_2-**2**	−153.3	−149.8	28.1	28.3
4- NO_2-**2**	−132.8	−128.2	7.6	6.7
5- NO_2-**2**	−156.4	−153.3	31.2	31.8
6- NO_2-**2**	−129.3	−124.8	4.1	3.3
7- NO_2-**2**	−125.8	−121.2	0.6	−0.3

⋆ Isotropic absolute shielding constants were calculated using the GIAO protocol at the DFT/aug-cc-pVDZ//DFT/aug-cc-pVDZ level of theory. During these calculations solvation corrections (CH_3CN for nitrobenzol, H_2O for all others) with the CPCM solvation model were performed at the same level of theory [21].

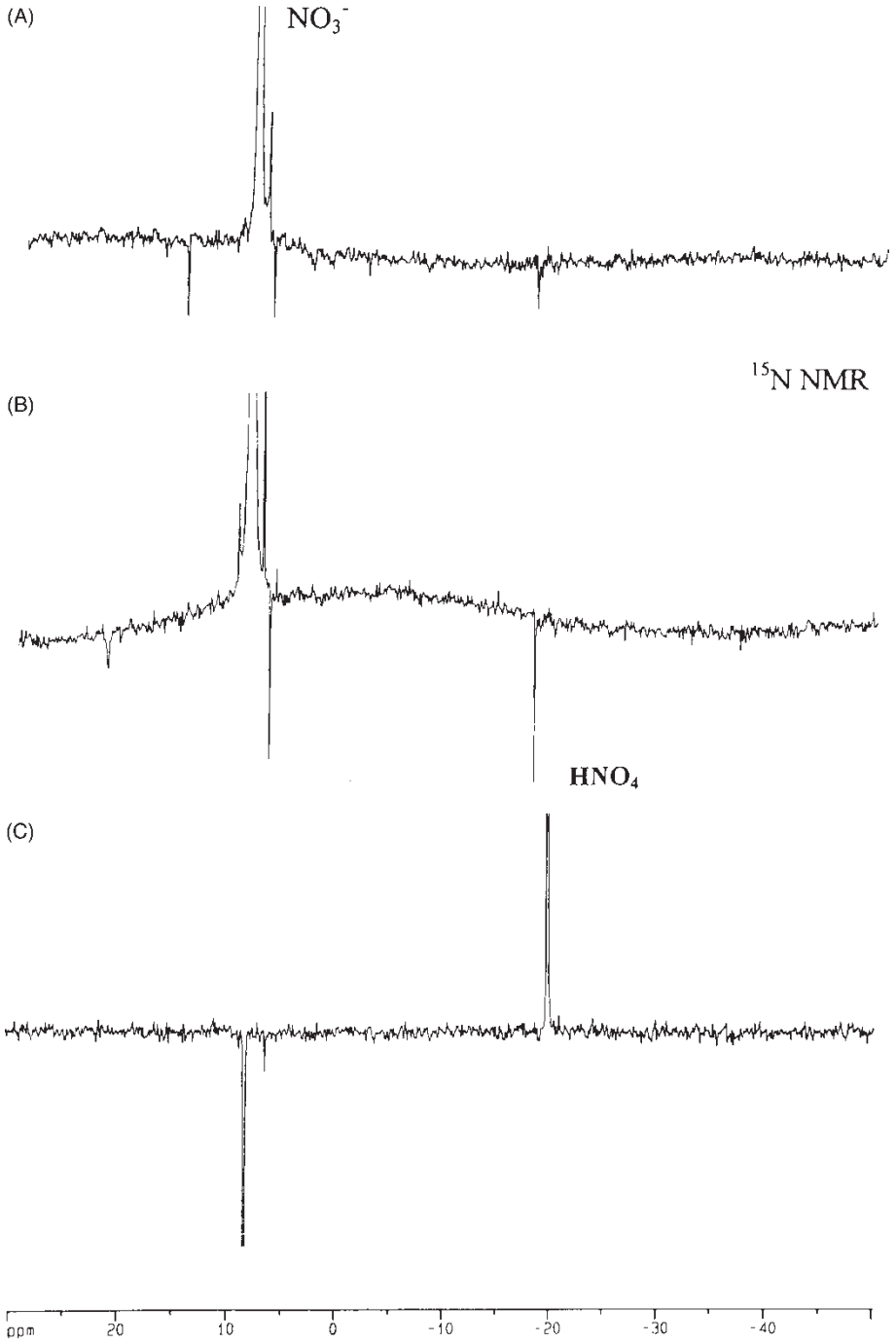

Figure 5. ^{15}N-NMR spectra of Mel in H_2O/D_2O 2 min after mixing the reactants (20 scans, delay time 20 s) with (A) peroxynitrite-^{15}N at pH 5, (B) peroxynitrite-^{15}N with $NaHCO_3$ at pH 5, (C) $H^{15}NO_4$ at pH 2.

signal at $\delta = -19$ ppm is due to $H^{15}NO_4$ and observed in the absence of Mel, too. Additionally, two emission signals at $\delta = 6$ ppm and $\delta = 16$ ppm only appear in the presence of Mel. The first one is assigned to 4-$^{15}NO_2$-Mel. For supporting this, a quantum-chemical calculation of ^{15}N chemical shifts has been performed with 3-methyl-5-methoxy-indane **2** as a model compound (Table VI), giving $\delta = 6.6$ ppm for 4-$^{15}NO_2$-**2**. The second one was not assigned; it might be due to 3- or 5-$^{15}NO_2$-Mel. In the presence of $NaHCO_3$, a similar spectrum was observed (Figure 5(A)). It does not show the signal at $\delta = 16$ ppm but another one at $\delta = 22$ ppm which was not assigned either. The ^{15}N-NMR signal of $^{15}NO_3^-$ appears in enhanced absorption as it was also observed in the absence of Mel.

During reaction of $H^{15}NO_4$ with Mel, the spectrum given in Figure 5(C) was taken showing the ^{15}N-NMR signals of $^{15}NO_3^-$ and of $H^{15}NO_4$ in enhanced absorption and emission. The signal at $\delta = 6$ ppm

$$\text{Mel} + {}^{15}NO_2^{\cdot} \rightarrow \text{Mel}^{\cdot} + H^{+} + {}^{15}NO_2^{-}$$

$$\text{Mel}^{\cdot} + {}^{15}NO_2^{\cdot} \rightarrow [\text{Mel}^{\cdot}, {}^{15}NO_2^{\cdot}]^{F} \xrightarrow{c} 4\text{–}{}^{15}\underline{N}O_2\text{–Mel} \quad (E)$$

Scheme 8. ^{15}N-CIDNP during nitration of melatonin with RNS.

shows emission, too, which supports its assignment to 4-$^{15}NO_2$-Mel.

The ^{15}N-CIDNP effects in $^{15}NO_3^-$ and $H^{15}NO_4$ are explained as described, see Schemes 4 and 5. The emission-type effect in the ^{15}N-NMR signal of 4-$^{15}NO_2$-Mel is explained in the same manner as those observed in $^{15}NO_2$-Tyr and $^{15}NO_2$-Trp, see Scheme 8.

Conclusions

The appearance of ^{15}N-CIDNP during reaction of Trp, *N*-AcTrp and Mel with various nitrating systems indicates the radical character of the nitration. Formation of 6-NO_2-Trp might be used as an additional marker for the endogeneous intermediacy of RNS. Of course, the detection of endogenous 6-NO_2-Trp is more difficult than the detection of endogenous 3-NO_2-Tyr because of both the lower concentrations of Trp in proteins compared to Tyr and the well known electron transfer from tryptophanyl radicals to tyrosine [38] which should favor the formation of 3-NO_2-Tyr at the expense of 6-NO_2-Trp. Therefore, the presence of both 6-NO_2-Trp and 3-NO_2-Tyr would indicate the occurrence of a massive nitrative stress whereas the single detection of 3-NO_2-Tyr indicated "only" the intermediacy of nitrogen dioxide [39].

The ^{15}N-CIDNP results do not rule out the possibility of non-radical nitrations. 4-NO_2-Trp is formed as the only nitration product of Trp during reaction with a complex between *Deinococcus radiodurans* NOS and a tryptophanyl-tRNA synthetase [40]. The missing component of the nitration product 6-NO_2-Trp makes a different nitration mechanism likely.

References

[1] Baeyer A, Villiger D. Über die salpetrige Säure. Chem Ber 1993;34:755–762.

[2] Beckman JS, Beckman TW, Chen J, Marshall PA, Freeman BA. Apparent hydroxyl radical production by peroxynitrite: Implications for endothelial injury from nitric oxide and superoxide. Proc Natl Acad Sci USA 1990;87:1620–1624.

[3] Ohshima H, Friesen M, Brouet I, Bartsch H. Nitrotysosine as a new marker for endogeneous nitrosation and nitration of proteins. Food Chem Toxicol 1990;28:647–652.

[4] Ischiropoulos H, Zou L, Tsai M, Martin JC, Smith CD, Beckman JS. Peroxynitrite-mediated tyrosine nitration catalysed by superoxide dismutase. Arch Biochem Biophys 1992;298:431–437.

[5] Suzuki T, Mower HF, Friesen MD, Gilibert I, Sawa T, Ohshima H. Nitration and nitrosation of *N*-acetyl-L-tryptophan and tryptophan residues in proteins by various reactive nitrogen species. Free Radic Biol Med 2004;37:671–681.

[6] Yamakura F, Ikeda K. Modification of tryptophan and tryptophan residues in proteins by reactive nitrogen species. Nitric Oxide 2006;14:152–161.

[7] Lymar SV, Khairutdinov RF, Hurst JH. Hydroxyl radical formation by O—O bond homolysis in peroxynitrous acid. Inorg Chem 2003;42:5259–5266. Goldstein S, Lind J, Merenyi G. Chemistry of peroxynitrites as compared to peroxynitrates. Chem Rev 2005;105:2457–2470. Kirsch M, Korth HG, Wensing A, Sustmann R, de Groot H. Product formation and kinetic simulations in the pH range 1–14 account for a free-radical mechanism of peroxynitrite decomposition. Arch Biochem Biophys 2003;418:133–150.

[8] Lymar SV, Hurst JK. Rapid reaction between peroxonitrite ion and carbon dioxide: Implications for biological activity. J Am Chem Soc 1995;117:8867–8868.

[9] Butler AR, Rutherford TJ, Short DM, Ridd JH. Tyrosine nitration and peroxonitrite (peroxynitrite) isomerisation: ^{15}N CIDNP NMR studies. Chem Commun 1997;2000:669–670, Butler AR, Rutherford, TJ, Short DM, Ridd JH. Application of CIDNP to the nitration of *N*-acetyltyrosine and to some reactions of peroxynitrite. Nitric Oxide 2000;4:472–482.

[10] Lehnig M. Radical mechanisms of the decomposition of peroxynitrite and the peroxynitrite/CO_2 adduct and of reactions with L-tyosine and related compounds as studied by ^{15}N CIDNP. Arch Biochem Biophys 1999;368:303–318. Lehnig M, Kirsch M. ^{15}N CIDNP investigations of the peroxynitrite decay and nitration of *N*-acetyl-L-tyrosine. Helv Chim Acta, 2006;89:2144–2166.

[11] Bargon J, Fischer H. Kernresonanz-Emissionslinien während rascher Radikalreaktionen II. Chemisch induzierte dynamische Kernpolarisation. Z Naturforsch 1967;22a:1556–1962.

[12] Closs GL. A mechanism explaining nuclear spin polarisations in radical combination reactions. J Am Chem Soc 1969;91:4552–4554. Kaptein R. Simple rules for CIDNP. *Chem Commun* 1971; 732–733.

[13] Winter G, Shioyama H, Steiner U. ET quenching of dye triplets by NO_2^- and NO_3^-. A spin-orbit coupling effect on the radical yield. Chem Phys Lett 1981;81:547–552.

[14] Clemens AH, Ridd JH, Sandall PB. ^{15}N Nuclear polarisation in nitration and related reactions. Part.1. Mesitylene. J Chem Soc Perkin Trans 1984;2:1659–1665.

[15] Lehnig M, Kirsch M. ^{15}N CIDNP investigations of the peroxynitric acid nitration of L-tyrosine and of related compounds. Org Biomol Chem 2006;4:721–729.

[16] Peyrot F, Martin MT, Migault J, Ducrocq C. Reactivity of peroxynitrite with melatonin as a function of pH and CO_2 content. Eur J Org Chem 2003;:172–181.

[17] Uppu RM, Pryor WA. Synthesis of peroxynitrite in a two-phase system using isoamyl nitrite and hydrogen peroxide. Anal Biochem 1996;236:242–249.

[18] Lehnig M. ^{15}N CIDNP during reaction of *N*-acetyl-L-tyrosine with the nitrating systems HRP/H_2O_2/NO_2^- and HOCl/NO_2^-. Arch Biochem Biophys 2001;393:245–254.

[19] Lehnig M. ^{15}N CIDNP during reaction of the oxoperoxonitrate-CO_2 adduct with bovine albumin and L-tyrosine derivatives. J Chem Soc Perkin Trans 2000;2:2016–2021.

[20] Lehnig M, Kirsch M, Korth HG. ^{15}N CIDNP study of formation and decay of peroxynitric acid: Evidence for formation of hydroxyl radicals. Inorg Chem 2003;42:4275–4287.

[21] Cheeseman JR, Trucks G, Keith TA, Frisch MJ. A comparison of models for calculating nuclear magnetic resonance shielding tensors. J Chem Phys 1996;104:5497–5509.

[22] Padmaja S, Ramazenian MS, Bounds PL, Koppenol WH. Reaction of peroxynitrite with L-tryptophan. Redox Rep 1996;2:173–177.

[23] Alvarez B, Rubbo H, Kirk M, Barnes S, Freeman BA, Radi R. Peroxynitrite-dependent tryptophan nitration. Chem Res Toxicol 1996;9:390–396.
[24] Herold S. Nitrotyrosine, dityrosine, and nitrotryptophan formation from metmyoglobin, hydrogen peroxide, and nitrite. Free Radic Biol Med 2004;36:565–579.
[25] Sala A, Nicolis S, Roncone R, Casella L, Monzani E. Peroxidase catalysed nitration of tryptophan derivatives. Eur J Biochem 2004;271:2841–2851.
[26] Lehnig M. Nitration of dimethoxybenzenes, mesitylene and toluene with nitric acid and mixed acid as studied by ^{15}N CIDNP. J Chem Soc Perkin 1966;2:1943–1948.
[27] Remers WA. Indoles, part one. In: Houlihan WJ, editor. The chemistry of heterocyclic compounds. New York: John Wiley & Sons; 1972. pp. 78–84.
[28] Harriman A. Further comments on the redox potentials of tryptophan and tyrosine. J Phys Chem 1987;91:6102–6104.
[29] Morton JR, Preston KF, Strach SJ. Paramagnetic oxides of nitrogen observed in a sulfur-hexafluoride matrix. J Phys Chem 1979;83:533–537.
[30] Lendzian F, Sahlin M, MacMillan F, Bittl R, Fiege R, Pötsch S, Sjöberg BM, Gräslund A, Lubitz W, Lassmann G. Electronic structure of neutral tryptophan radicals in ribonucleotide reductase studied by ERP and ENDOR spectroscopy. J Am Chem Soc 1996;118:8111–8120.
[31] Posener ML, Adams GE, Wardman P. Mechanism of tryptophan oxidation by some inorganic radical-anions. A pulse radiolysis study. J Chem Soc Faraday Trans 1996; 72:2231–2238.
[32] Himo F, Eriksson LA. Theoretical study of model tryptophan radicals and radical cations. Comparison with experimental data of DNA photolyase, cytochrome c peroxidase, and ribonucleotide reductase. J Phys Chem B 1997; 101:9811–9819.
[33] Schweitz D, Spiess HW. ^{15}N-NMR of pyridine in high magnetic fields. J Magn Reson 1974;15:529–539.
[34] Koppenol WH, Moreno JJ, Pryor WA, Ischiropoulos H, Beckman JS. Peroxynitrite, a cloaked oxidant formed by nitric oxide and superoxide. Chem Res Toxicol 1992;5:834–842, Coddington JW, Hurst JK, Lymar SV. Hydroxyl radical formation during peroxynitrous acid decomposition. *J Am Chem Soc* 1999,121:2438–2443.
[35] Pfeiffer S, Gorren AC, Schmidt K, Werner ER, Hansert B, Bohle DS, Mayer B. Metabolic fate of peroxynitrite in aqueous solution. J Biol Chem 1977;272:3465–3470.
[36] Shibata H, Kono Y, Yamashita S, Sawa Y, Ochiai H, Tanaka K. Degradation of chlorophyll by nitrogen dioxide generated from nitrite by the peroxidase reaction. Biochem Biophys Acta 1995;1230:45–50.
[37] van der Vliet A, Eiserich JP, Halliwell B, Cross CE. Formation of reactive nitrogen species during peroxidase-catalysed oxidation of nitrite. J Biol Chem 1997;272:7617–7625.
[38] Butler J, Land EJ, Prütz WA, Swallow AJ. Charge transfer between tryptophan and tyrosine in proteins. Biochim Biophys Acta 1982;705:150–162.
[39] Kirsch M, Korth HG, Sustmann R, de Groot H. The pathobiochemistry of nitrogen dioxide. Biol Chem 2002;383:389–399.
[40] Buddha KM, Tao T, Parry RJ, Crane B. Regioselctive nitration of tryptophan by a complex between bacterial nitric-oxide synthase and tryptophanyl-tRNA synthetase. J Biol Chem 2004;279:49567–49570.